AIAA AVIATION Forum
5-9 June 2017, Denver, Colorado
35th AIAA Applied Aerodynamics Conference

10.2514/6.2017-4077

Design Methodology for a Dynamically-Scaled General Aviation Aircraft

Gavin K. Ananda*, Moiz Vahora†, Or D. Dantsker‡, and Michael S. Selig§
Department of Aerospace Engineering, University of Illinois at Urbana–Champaign, Urbana, IL 61801, USA

This paper discusses the motivation, requirements, and approach of the University of Illinois at Urbana-Champaign (UIUC) General Aviation Upset and Stall Testing Aircraft Research (GA-USTAR) project. The goal of the GA-USTAR project is to build and flight test a dynamically-scaled, Reynold number corrected model of a General Aviation (GA) type aircraft intended for upset and stall flight modeling. The project is separated into three phases. In Phase 1, to simplify the construction, a scaled commercial-of-the-shelf radio control (R/C) model of a GA aircraft is used as a starting point. From a list of available GA aircraft R/C models, a 1/5-scale Cessna 182 was selected. The methodology behind the choice of the Cessna 182 as the GA-USTAR Phase 1 (baseline) model is detailed. The method of accurately determining the mass distribution and inertias is described in detail. In Phase 2, the approach taken to appropriately dynamically scale the Phase 1 Cessna 182 model is discussed. The desired geometric, kinematic, and mass parameters for a dynamically-scaled Cessna 182 is discussed. Finally, to ensure that stall is closely matched, new airfoils will be designed and tested in the UIUC subsonic wind tunnel and then used on the GA-USTAR Phase 3 flight platform. New airfoils are required to correct for the Reynolds number effects inherent in scaled models. Flight testing and data acquisition will be performed for all three phases of the GA-USTAR project. Details regarding flight data instrumentation and flight test planning are also described in this paper.

Nomenclature

AR	=	aspect ratio
a	=	acceleration (ft/s^2)
b	=	wingspan (ft)
c	=	chord (ft)
C_l	=	airfoil lift coefficient
$C_{l_{max}}$	=	airfoil maximum lift coefficient
C_L	=	surface lift coefficient ($= L/\frac{1}{2}\rho V_\infty^2 S_{ref}$)
$C_{m_{c/4}}$	=	airfoil moment coefficient at quarter chord
$C_{M_{c/4}}$	=	surface moment coefficient at quarter chord ($= M'/\frac{1}{2}\rho V_\infty^2 S_{ref} c$)
D	=	drag (lb)
E	=	tensile and compressive modulus of elasticity (lb/ft^2)
EI'	=	bending stiffness (lb-ft^2)
F	=	force (lb)
Fr	=	Froude number

*Graduate Student (Ph.D. Candidate), 104 S. Wright St., AIAA Student Member. anandak1@illinois.edu
†Undergraduate Research Assistant, 104 S. Wright St., AIAA Student Member. mvahor2@illinois.edu
‡Graduate Student (Ph.D. Candidate), 104 S. Wright St., AIAA Student Member. dantske1@illinois.edu
§Professor, 104 S. Wright St., AIAA Associate Fellow. m-selig@illinois.edu

G	=	shear modulus of elasticity (lb/ft^2)
GJ'	=	torsional stiffness (lb-ft^2)
g	=	acceleration of gravity (ft/sec^2)
I_{XX}, I_{YY}, I_{ZZ}	=	principal moments of inertia (slug-ft^2)
J'	=	second torsional moment of inertia (ft^4)
l	=	characteristic dimension (ft)
L	=	lift (lb)
m	=	mass (slug)
M	=	Mach number
M'	=	moment (lb-ft)
Re	=	Reynolds number based on mean aerodynamic chord (= $V_\infty c/\nu$)
s	=	linear displacement (ft)
S_{ref}	=	reference area (ft^2)
Str	=	Strouhal number
T	=	torque (lb-ft)
V_∞	=	freestream velocity (ft/s)
α	=	angle of attack (deg)
α'	=	aerodynamic attitude (deg)
β	=	sideslip angle (deg)
δ	=	control surface deflection angle (deg)
ϕ'	=	angular displacement (deg)
ρ	=	density of air (slugs/ft^3)
τ	=	reduced time parameter
ν	=	kinematic viscosity (ft^2/sec)
Ω	=	angular rate (rad/sec)
$\dot{\Omega}$	=	angular acceleration (rad/sec^2)
ω	=	frequency of oscillation (rad/sec)

Subscripts

DS	=	dynamically-scaled
FS	=	full-scale

Acronyms

$COTS$	=	commercial-of-the-shelf
GA	=	general aviation
R/C	=	radio control
$FSTD$	=	flight simulation training device

I. Introduction

The FAA and the European Aviation Safety Agency recently proposed new rules[1–3] regarding the use of enhanced Flight Simulation Training Devices (FSTD) for special hazard training such as loss of control. Flight simulator manufacturers are required to properly model stall and upset recovery situations, and that they be valid for at least 10 deg beyond the stall angle of attack. Validation of flight simulator models are typically performed against actual flight test data for a specific aircraft (type-specific aerodynamic model). An alternative approach proposed in this project is to use a smaller dynamically-scaled model that both matches the aerodynamic properties, kinematics, and weight distributions of the full-scale aircraft. In this way, all necessary stall/upset maneuvers can be peformed without the risks associated with potential human loss and cost overruns. The resulting aerodynamic model would be type-representative (based on best practices of flight modeling from analytical and empirical means) in the stall/post-stall regime.

Scaled aircraft models have been used to design and test new aircraft configurations since the development of the Wright Flyer.[4] As these scaled models developed, they were often used to simulate the dynamics and aerodynamics of aircraft safely and cost effectively. Wolowicz, et al.[5] discussed how simply scaling an aircraft and testing is not enough to accurately simulate the motions of these aircraft as the dynamics and aerodynamics differ vastly since weight and Reynolds number differ. This fact thereby requires correction factors to be employed before any data can be used. Two of the most common methods of testing scaled models are the static models tested inside wind tunnels and free-flying models that are flown. Experiments with stationary models are useful for modeling aerodynamics and are easier to control than free-flying models, but one of their inherent limitations is its inability to model aircraft dynamics, while free-flying models are capable of modeling the motions and aerodynamics of aircraft. A dynamically-scaled model is a free flying scaled model capable of simulating the motions of a full-scale aircraft while costing less and being safer.

Currently, dynamically-scaled vehicles have been used for the improvement of commercial transport stall models through the NASA Airborne Subscale Transport Aircraft Research (AirSTAR) Program.[6–9] Although in the past dynamically-scaled models have been used in General Aviation (GA) research (NASA Stall/Spin Research Program[10,11]), more recently, however there has not been substantial programs in GA for stall/upset modeling and research. This is a critical issue that needs to be addressed since, according to the National Transportation and Safety Board (NTSB) Review of Civil Aviation Accidents from 2010[12] and the NTSB 2015/2016/2017 Most Wanted Transportation Safety Improvements factsheets,[13–15] fixed-wing general aviation (GA) accidents accounted for 89% of all accidents and 86% of total fatalities of U.S. civil aviation, where loss of control accounted for approximately 48% of these fatal accidents (between 2008 to 2014).

This paper focuses on the approach and development of the General Aviation Upset and Stall Testing Aircraft Research (GA-USTAR) project at UIUC. The objective of the GA-USTAR project is to provide validation data sets for upset/stall aerodynamic model development for GA aircraft.[16] To accomplish this task, the GA-USTAR project is divided into three phases. In Phase 1, a baseline commercial-of-the-shelf (COTS) scaled model of a GA aircraft is selected, fully instrumented, and flight tested.[17] In Phase 2, the baseline model is dynamically scaled to ensure mass distribution similarities to the full-scale GA aircraft. The final phase of the GA-USTAR project (Phase 3) requires the design of a new wing with airfoils whose stall curve characteristics match full-scale aircraft stall curve characteristics despite the Reynolds number differences observed.

This paper is arranged as follows. First, the dynamic scaling methodology and approach is described in detail. Next, each of the phases of the GA-USTAR project are discussed. Finally, the instrumentation of the GA-USTAR aircraft and flight goals are discussed.

II. Dynamic Scaling Methodology

Type-specific pre-stall aerodynamic models are generally created by validating against full-scale aircraft flight-test data. It is however highly risky and expensive to perform stall/upset manuevers using a full-scale aircraft. An alternative approach proposed is to use a smaller dynamically-scaled model that in non-dimensional terms both matches the aerodynamic properties and weight distributions of the full-scale aircraft. In this way, all necessary upset maneuvers can be peformed without the risks associated with potential human loss and cost overruns. The resulting aerodynamic model would be type-representative in the stall/post-stall regime.

As a result, one of the objectives of this project is to perform stall/upset maneuvers using a dynamically-scaled test platform that is fully equipped with a sensor and flight computer package that accurately measures and logs the state of the aircraft in flight. The UIUC Aero Testbed,[18,19] a 35% scale Extra 260 (Fig. 1) has been used to perform various stall/post-stall maneuvers. The test aircraft contained a full sensor array package (inertial measurement unit, GPS, potentiometers, etc.) and flight computer to determine the state of the aircraft in flight with high fidelity. It is, however, not dynamically scaled and as a result will not accurately match the flying qualities of a full-scaled aircraft.

A dynamically-scaled model is a free-flying scaled aircraft model that is capable of simulating the relative motions of a larger full-scale aircraft. This means that in a proportional period of time, the scaled model would react in a similar manner to external flow conditions as the full-scale model (i.e., flight path and angular displacements match based on scaling laws).[5] As per Ref. 5, dynamic scaling is performed by

Figure 1. Photograph of the 35% scale Extra 260 UIUC Aero Testbed. [18,19]

matching certain non-dimensional similitude parameters of the scaled model to the full-size aircraft. The dimensional parameters affecting the forces (F) and moments (M') on an aircraft are,

$$F = f\left(\rho, \mu, V_s, l, \alpha', V, a, \delta, \Omega, \dot{\Omega}, \omega, g, t, m, I, EI', GJ'\right) \tag{1}$$

$$M' = f\left(\rho, \mu, V_s, l, \alpha', V, a, \delta, \Omega, \dot{\Omega}, \omega, g, t, m, I, EI', GJ'\right) \tag{2}$$

From dimensional analysis, the dimensional parameters are nondimensionalized to become

$$\frac{F}{\frac{1}{2}\rho V^2 l^2} = f(\alpha', \delta, \frac{\Omega l}{V}, \frac{\Omega l^2}{V^2}, \frac{al}{V^2}, \frac{\omega l}{V}, \frac{\rho V l}{\mu}, \frac{V^2}{lg}, \frac{V}{V_S}, \frac{m}{\rho l^3}, \frac{I}{\rho l^5}, \frac{EI'}{\rho V^2 l^4}, \frac{GJ'}{\rho V^2 l^4}, \frac{tV}{l}) \tag{3}$$

$$\frac{M'}{\frac{1}{2}\rho V^2 l^3} = f(\alpha', \delta, \frac{\Omega l}{V}, \frac{\Omega l^2}{V^2}, \frac{al}{V^2}, \frac{\omega l}{V}, \frac{\rho V l}{\mu}, \frac{V^2}{lg}, \frac{V}{V_S}, \frac{m}{\rho l^3}, \frac{I}{\rho l^5}, \frac{EI'}{\rho V^2 l^4}, \frac{GJ'}{\rho V^2 l^4}, \frac{tV}{l}) \tag{4}$$

where the non-dimensional similitude parameters are listed in Table 1. Realistically, not all similarity parameters listed in Table 1 are required or are capable of being matched. Given that most full-scale GA aircraft fly at Mach numbers lower than 0.3, the incompressible flow assumption can be maintained. This means that Mach number scaling is not necessary here. In addition, the aircraft is assumed to be aeroelastically rigid, thereby removing the need to match aeroelastic bending and torsion parameter scaling requirements.

Table 2 lists all the critical scaling factors derived from the similitude parameters in Table 1. The factors are separated into geometric, inertial, and kinematic scaling relations. The scale factors are determined as follows. Firstly, the scale factors required to perform geometric and mass scaling are determined. The scaled model will be geometrically scaled by a factor of n. As a result all lengths of the aircraft are scaled by a factor of n and consequently all areas are scaled by a factor of n^2. The dynamically-scaled model will also fly at a lower altitude in cruise compared with the full-scale aircraft. The cruise altitude difference between the dynamically-scaled (DS) and full-scale (FS) aircraft is related by the relative density scale factor of

$$\sigma = \frac{\rho_{DS}}{\rho_{FS}} \tag{5}$$

Both n and σ are used to determine the required mass scaling. The relative mass density parameter is used where

$$\frac{m_{FS}}{\rho_{FS} S_{FS} c_{\bar{FS}}} = \frac{m_{DS}}{\rho_{DS} S_{DS} c_{\bar{DS}}} \tag{6}$$

Rearranging the equations and introducing n and σ, the mass scaling factor is related by

$$\frac{m_{DS}}{m_{FS}} = \frac{\rho_{DS}}{\rho_{FS}} \frac{S_{DS}}{S_{FS}} \frac{c_{\bar{DS}}}{c_{\bar{FS}}} = \sigma n^3 \tag{7}$$

Table 1. Similitude Parameters

Parameter	Equation
Angular Velocity Parameter	$\frac{\Omega l}{V}$
Reduced Angular Acceleration	$\frac{\Omega l^2}{V^2}$
Reduced Linear Acceleration	$\frac{al}{V^2}$
Strouhal Number, Str	$\frac{\omega l}{V}$
Reynolds Number, Re	$\frac{\rho V l}{\mu}$
Froude Number, Fr	$\frac{V^2}{lg}$
Mach Number, M	$\frac{V}{V_S}$
Relative Density Factor	$\frac{m}{\rho l^3}$
Relative Mass Moment of Inertia	$\frac{I}{\rho l^5}$
Aeroelastic Bending Parameter	$\frac{EI'}{\rho V^2 l^4}$
Aeroelastic Torsion Parameter	$\frac{GJ'}{\rho V^2 l^4}$
Reduced Time Parameter	$\frac{tV}{l}$

Table 2. Derived Scale Factors based on Similitude Parameters

Parameter	Symbol	Scaling Factor
Geometric		
Length	l	n
Density	ρ	σ
Inertial		
Mass	m	σn^3
Moment of Inertia	I	σn^5
Kinematic		
Time	t	$\sqrt{n}$
Velocity	V	$\sqrt{n}$
Attitude	α'	1
Control Surface Deflection	δ'	1
Angular Rate	Ω	$1/\sqrt{n}$
Angular Displacement	ϕ'	1
Angular Acceleration	$\dot{\Omega}$	$1/n$
Linear Displacement	s	n
Linear Acceleration	a	1
Oscillatory Frequency	ω	$1/\sqrt{n}$

Similarly, the moment of inertia scaling factor is determined from the relative mass moment of inertia parameter to be

$$\frac{I_{DS}}{I_{FS}} = \frac{\rho_{DS}}{\rho_{FS}} \frac{l_{DS}^5}{l_{FS}^5} = \sigma n^5 \tag{8}$$

Looking at the kinematic scaling factors for the aircraft, flight velocity is scaled based on the Froude number similarity parameter by

$$\frac{V_{DS}}{V_{FS}} = \sqrt{\frac{l_{DS}}{l_{FS}} \frac{g}{g}} = \sqrt{n} \tag{9}$$

The other scaling factors are determined in a similar manner and are listed in Table 2. Note that from Table 1, only the Reynolds number, Mach number, aeroelastic bending parameter, and aeroelastic torsion parameters were not used for the scaling factor derivations listed in Table 2.

The scale factors developed in Table 2 exhibit that while using a dynamically-scaled aircraft is safer and more cost-effective than a full-scale aircraft, there are stringent requirements to properly dynamically scale an aircraft. These issues relate to the mass and moment of inertias required to perform proper scaling. A scaled aircraft mass will have to be scaled by the cube of the scale factor while also scaling by the fifth power of the inertia. Also, the angular velocities of the dynamically-scaled model would have to exhibit would be $1/\sqrt{n}$ times that of the full-scale aircraft.

The key relationships observed when dynamically scaling an aircraft are presented in Figs. 2(a–d). These were adapted using similar methods to that developed by Ref. 5. All plots in Figs. 2(a–d) are for n varying from 0.1 to 0.3 in 0.05 increments. Figures 2(b–d) have σ in the y-axis. Figures 2(a–b) has the mass scale factor in the x-axis. Example cases in red, blue, and black are shown in the plots to illustrate the relationships between these parameters. Starting from Fig. 2(d), σ increases with increasing full-scale aircraft cruise altitude and is not affected by change in n. An increase in σ (due to increased flight altitude) corresponds then to an increase in dynamic pressure ratio (q_{DS}/q_{FS}) when n is maintained constant as seen in Fig. 2(c). The dynamic pressure ratio also increases with n. The effect of n and σ on the mass scale factor (m_{DS}/m_{FS}) is shown in Fig. 2(b) where a 5,000 ft increase in flight altitude minimally increases the mass scale factor in comparison with an increase of n by 0.1. Similarly, from Fig. 2(a), n has a much larger impact on the inertia scale factor (I_{DS}/I_{FS}). What is evident is that the geometric scale factor has a much more prominent impact on the mass and inertias of the dynamically scaled aircraft. An increase in full-scale aircraft cruise altitude by 5,000 ft minimally changes both the required mass and inertia of the dynamically-scaled aircraft.

An example of a dynamically-scaled model is the NASA AirSTAR which is a 5.5% scale model of a general transport model (GTM) aircraft that wa used to research the motions of commercial transport aircraft flying outside of their flight envelopes.[6–9] The NASA AirSTAR was designed using the same scaling laws in Table 2, with the dynamically-scaled model matching the inertias by 3% and weight by 0.1%. Using the CAD model, the manufacturers of the GTM were able to determine the flight time, battery, payload, and data system requirements of the model and they were able to also determine the effects of adding loading to the fuselage by applying the scaling laws to the C.G. envelope of the GTM.[20]

III. GA-USTAR Project Phases

As discussed prior, the GA-USTAR project is divided into three phases. This section describes each of these phases of the project with the goal of obtaining a dynamically-scaled, Reynolds number corrected aircraft that can be used for stall/upset flight data collection.

A. Phase 1

1. Aircraft Selection

To design and build a dynamically-scaled GA model for the GA-USTAR project, detailed research was conducted into the various full-scaled aircraft to possibly scale. Factors taken into account were common full-scale aircraft configurations, the availability of full-scale geometric data (including inertias), the availability of commercial-of-the-shelf (COTS) R/C models that were geometrically (but not dynamically) similar,

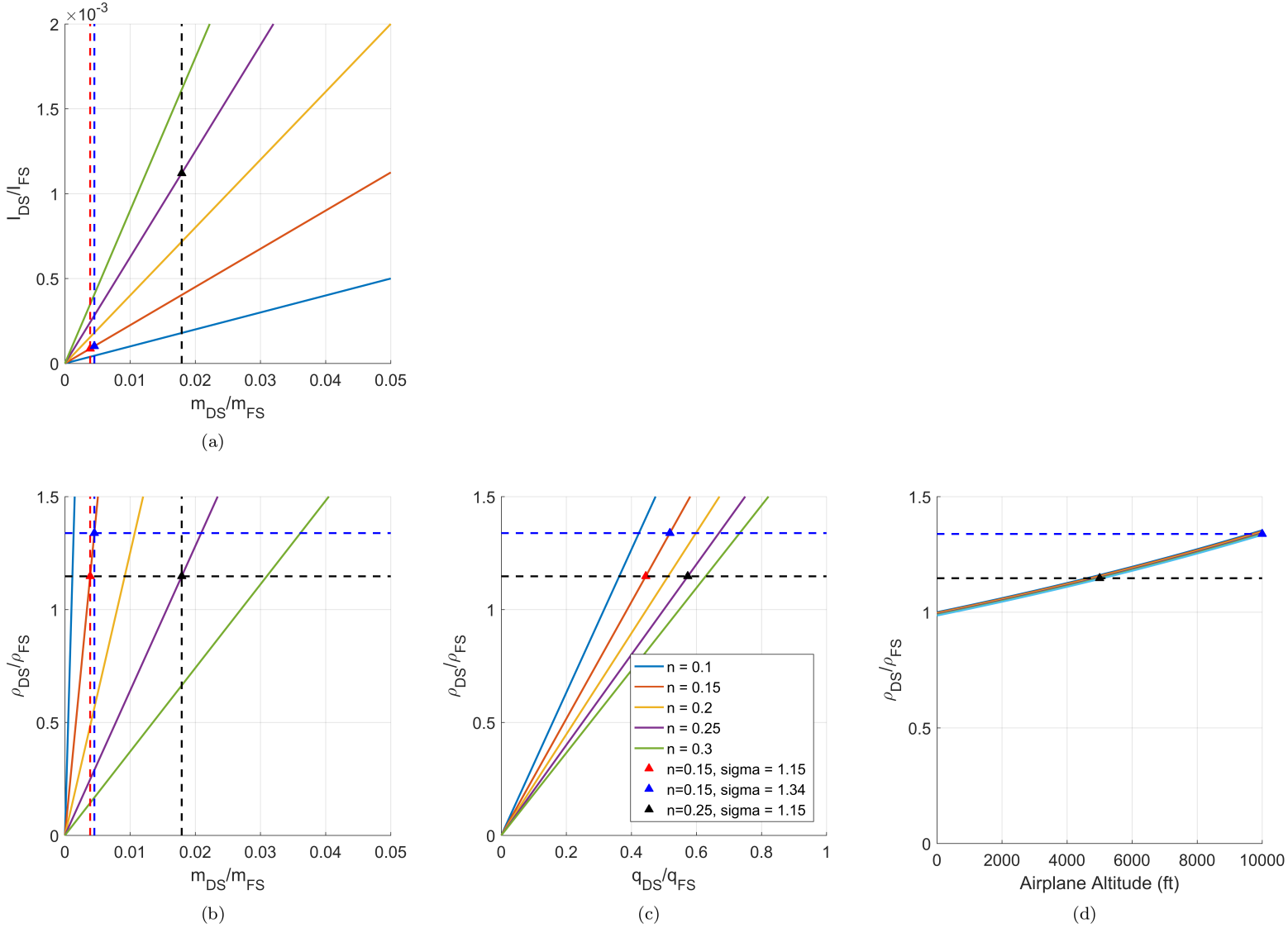

Figure 2. Key scale factor relationships when dynamically scaling an aircraft: (a) I_{DS}/I_{FS} vs m_{DS}/m_{FS}, (b) ρ_{DS}/ρ_{FS} vs m_{DS}/m_{FS}, (c) ρ_{DS}/ρ_{FS} vs m_{DS}/m_{FS}, and (d) I_{DS}/I_{FS} vs m_{DS}/m_{FS}.

knowledge of the aerodynamic (airfoils used) properties of the full-scale aircraft, FAA regulations (flight altitude and weight limitations), and finally practicality of scaling in terms of mass and mass distributions compared with the R/C model.

A list of potential aircraft were compiled along with their corresponding scaled COTS R/C models that may be modified into a dynamically-scaled model. Using the known weights and wingspan for each aircraft and the wingspan of each corresponding COTS R/C model, the weight of its dynamically-scaled model was calculated using the relations described in Table 2. A plot comparing the dynamically-scaled and COTS weight for the potential aircraft is shown in Fig. 3, where a full-scale altitude of 5,000 ft and a model altitude of 350 ft was used to calculate the density scaling factor σ. Note that in order to comply with FAA regulations, which limit the altitude of civilian unmanned aerial vehicles (UAVs) to 400 ft, the density scaling factor was modified such that the model flies at 350 ft. The results in Figure 3 reiterate results from trade studies in the prior section in that the COTS R/C models require additional weight in order to transform them into dynamically-scaled models.

The weight necessary for the dynamically-scaled models to comply with FAA regulations (55 lb limit) required that the COTS R/C scaled model choices be limited to between the 1/4th- and 1/5th-scaled GA aircraft. The aircraft list was then narrowed down to the aircraft described in Table 3. The table lists the dynamically-scaled weights of each aircraft choice and the % weight difference between the COTS R/C model and the dynamically-scaled model. From Table 3, it was evident that the Piper J-3 Cub COTS R/C

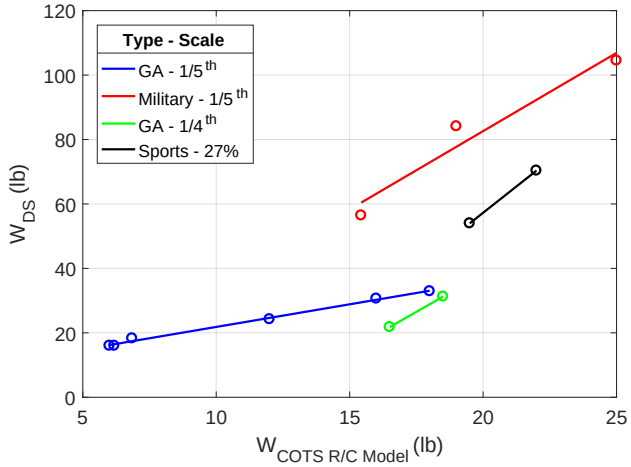

Figure 3. COTS R/C Model vs. dynamically-scaled model weight.

Table 3. Dynamically-Scaled Aircraft Choices

Aircraft	**Cessna 182**	**Cirrus SR22T**	**PA-18 Super Cub**	**Piper J-3 Cub**
COTS R/C Model	1/5-Scale Top Flite Cessna 182	Hangar 9 Cirrus SR22T 30cc ARF	1/4-Scale Hangar 9 PA-18 Super Cub	1/4-Scale Hangar 9 J-3 Cub
Full scale weight (lb)	2,650	3,600	1,750	1,220
Full scale wingspan (ft)	36	38	35	35.25
COTS R/C model weight (lb)	12.5	18	18.5	16.5
COTS R/C model wingspan (ft)	6.75	8.07	8.83	8.83
n	0.188	0.212	0.252	0.250
σ	1.149	1.149	1.149	1.149
Dynamically-scaled weight (lb)	20.07	39.61	32.28	22.03
Weight difference (%)	60.5	120.0	74.5	33.5

Table 4. Cessna 182 A/B/C Details

Geometric Properties		
Overall Length	29	ft
Wingspan	36	ft
Wing Area	174	ft^2
Mean Chord	4.8	ft
Wing Aspect Ratio	7.47	
Weight		
Gross Weight [MAX]	2650	lb
Gross Weight [MIN]	2260	lb
Inertias		
I_{XX}	948	slug ft^2
I_{YY}	1,346	slug ft^2
I_{ZZ}	1,967	slug ft^2

Altitudes		
$h_{cruise,min}$	5000	ft
$h_{cruise,max}$	10000	ft
h_{land}	1000	ft
Speed		
Cruise Speed @ 7,000 ft	244.73	ft/s
Stall Speed, Clean	91.14	ft/s
Stall Speed, Full Flaps	82.70	ft/s
Reynolds Number		
$Re_{cruise,min}$	6.66E+06	
$Re_{cruise,max}$	5.87E+06	
$Re_{stall,clean}$	2.74E+06	
$Re_{stall,full-flaps}$	2.48E+06	
Lift Coefficient		
$C_{L,cruise,min}$	0.23	
$C_{L,cruise,max}$	0.27	
$C_{Lmax,stall}$ [W_E, clean]	1.35	
$C_{Lmax,stall}$ [W_E, full-flaps]	1.65	

model weight was closest to the dynamically scaled weight. Upon further research however, the Cessna 182 was chosen to be scaled and a 1/5th-scale Top Flite Cessna 182 Skyline Flight R/C model was purchased as the GA-USTAR platform. One of the primary reasons that the Cessna 182 was chosen is the wide availability of mass distribution and inertia data in literature[21,22] which is required to scale the geometric and mass properties of the aircraft. Note that the Cessna 182 aircraft variant chosen was the A/B/C variants. These were the variants that had aircraft inertias and mass distribution data available in literature.[22] Key information for the Cessna 182 A/B/C variants are shown in Table 4.

2. Inertia Measurements

Prior to moving to Phase 2, it was critical that accurate mass and inertia properties of the Phase 1 (baseline) GA-USTAR aircraft were obtained. These properties would help determine the necessary geometric and mass distribution modifications for the Phase 1 aircraft. As a result, a detailed CAD model was created for the purpose of matching the exact weight distributions of the baseline aircraft. The CAD model is shown in Fig. 4. The CAD model included all structural members of the wing, fuselage, horizontal tail, and empennage together with the full suite of electronic equipment and instrumentation used on the aircraft.

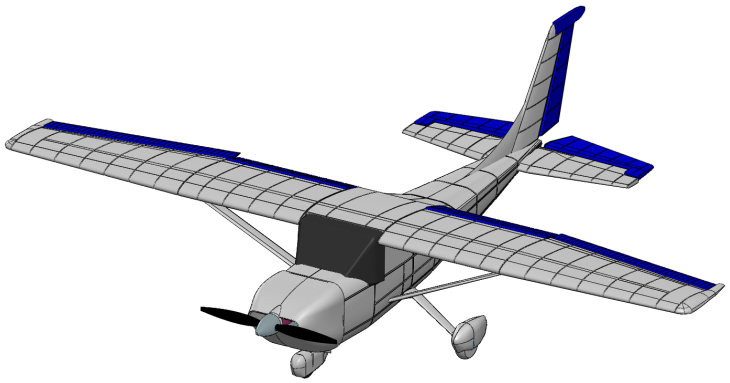

Figure 4. Isometric view of Cessna 182 model.

Table 5. 1/5-Scale Top Flite Cessna 182 COTS Model Details

Geometric Properties		
Overall Length	5.33	ft
Wingspan	6.75	ft
Wing Area	6.236	ft^2
Mean Chord	0.924	ft
Wing Aspect Ratio	7.47	
Weight		
Gross Weight [MAX]	15.31	lb
Gross Weight [MIN]	15.31	lb
Inertias		
I_{XX}	0.3560	slug ft^2
I_{YY}	0.4998	slug ft^2
I_{ZZ}	0.7395	slug ft^2

Direct inertia measurements of the baseline aircraft were necessary to validate the inertia values derived from the CAD model. These measurements were carried out using an inertia rig that measured the angular acceleration ($\dot{\Omega}$) about one of the pricipal axes of the baseline aircraft based on an input torque (T). The measurement method involved hanging a component of the baseline aircraft (wing or fuselage) about its principal axes and applying a known torque. The angular acceleration of the component about its principal axes was measured using an optical encoder. Given a known torque input and measured angular acceleration, the inertia of the component was calculated by

$$T = I\dot{\Omega} \tag{10}$$

The principal inertias (I_{XX}, I_{YY}, and I_{ZZ}) of the full baseline aircraft were calculated from the measured individual component inertias using parallel axis theorem. These measurements were used to adjust the CAD model results. As a result, the CAD model can be used to reassign the weight distributions and possibly redesign the wing and/or empennage to acheive the required weights for the GA-USTAR Phase 2 aircraft. Key details of the 1/5-scale Top Flite Cessna 182 (baseline aircraft) including preliminary values of the measured inertias are given in Table 5.

B. Phase 2

1. Scaling Requirements

A key issue when dynamically scaling an aircraft is that it tends to have a larger weight than the COTS R/C model weight. A method of minimizing the dynamically-scaled model weight is to scale weights based on the Cessna 182 in the low fuel state. As long as the aircraft stays within its C.G. envelope, the low fuel configuration would be a valid loading configuration. In addition, stall/upset events most commonly occur during the approach/landing phase of flight where fuel levels are usually low.

Given that the Cessna 182 is 2,650 lb with a full fuel load and approximately 2,200 lb with no fuel, a set of carpet plots were created as shown in Fig. 5. The carpet plots relate the dynamically-scaled model weight (W_{DS}) and inertias (I_{FS}) to the variation of full-scale weight (W_{FS}) and the aircraft cruising altitude (h_{cruise}). This approach helps elucidate the weight and inertia ranges that the dynamically scaled aircraft can be built to. In addition, Table 6 was created to detail all key minimum and maximum requirements of the dynamically-scaled Cessna 182.

2. Matching Approach

From literature of previous dynamically-scaled aircraft,[20] the main issue observed was that the dynamically-scaled I_{XX} inertia has large differences to the COTS R/C model I_{XX} due to the distribution of weight along the wing. As a result, dynamically-scaled aircraft wings have to be extremely lightweight to achieve the required values. For aircraft of this (R/C model) scale, there are predominantly two types of construction.

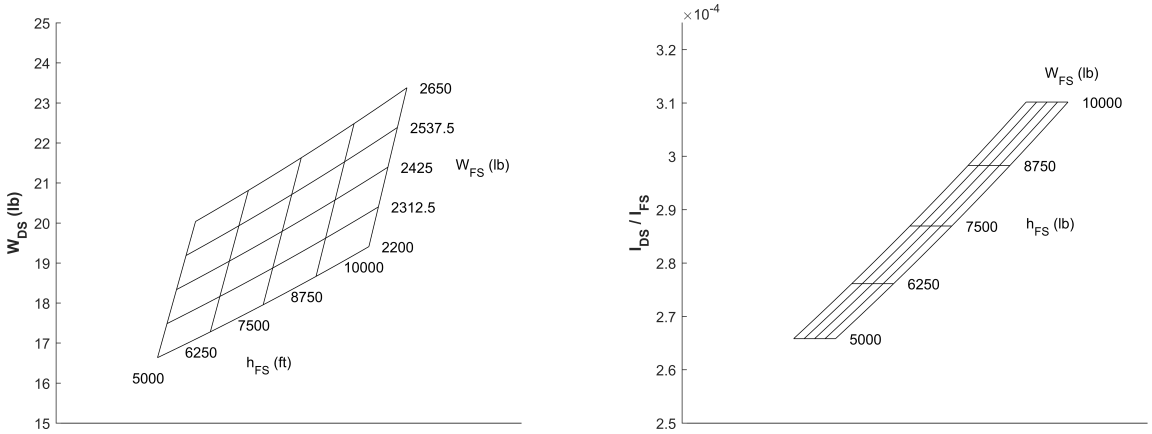

(a) (b)

Figure 5. Carpet plots showing the effect of varying full-scale aircraft flight altitude (h_{FS}) and weight (W_{FS}) on (a) W_{DS} and (b) I_{DS}/I_{FS} is shown.

Table 6. Minimum and Maximum Requirements of the Dynamically Scaled GA-USTAR Configuration

	Min, $h_{cruise,FS}$		**Max,** $h_{cruise,FS}$	
n	0.1875		0.1875	
Geometric Properties				
Overall Length	5.33	ft	5.33	ft
Wingspan	6.75	ft	6.75	ft
Wing Area	6.24	ft^2	6.24	ft^2
Mean Chord	0.92	ft	0.92	ft
Wing Aspect Ratio	7.47		7.47	
Altitudes				
h_{cruise}	350	ft	350	ft
h_{land}	100	ft	100	ft
σ	1.15		1.34	
Weight				
Gross Weight Cruise	20.07	lb	23.41	lb
Gross Weight Landing	17.11	lb	19.97	lb
Inertias				
I_{XX}	0.252	slug-ft^2	0.294	slug-ft^2
I_{YY}	0.358	slug-ft^2	0.418	slug-ft^2
I_{ZZ}	0.524	slug-ft^2	0.611	slug-ft^2
Speed				
Cruise Speed	105.97	ft/s	105.97	ft/s
Stall Speed, Flaps Up	39.47	ft/s	39.47	ft/s
Stall Speed, Flaps Down	35.81	ft/s	35.81	ft/s

Wings are either built-up of plywood and balsa structures, fully or partially sheeted with balsa, and then covered with a light plastic shrink wrap, or they have a composite structure with a monocoque skin, which is either carbon fiber, fiberglass, kelvar, or sandwich of composite cloth and light-weight filler (e.g., honeycomb or balsa).

In terms of pros and cons for each construction type, composite construction is generally lighter, yields

more rigid structures, and produces more accurate designs. Composites, however, are more expensive and difficult to repair. Wood built-up designs are relatively low cost, can easily be built, repaired, and modified but are not as rigid and heavier. Additionally wood does not have uniform density nor strength characteristics and is highly variable between pieces or even within a piece. Wooden designs also have the unique problem of bowing when exposed to a significant amount of sunlight, especially with dark-color film covering. Bowing is caused by the plastic film covering the wings: after being exposed to sunlight for a sufficient amount of time, the film heats up and contracts, and since only the top half of the aircraft receives sunlight the wings bend up. It should also be noted that there may be combinations of the two methods available, depending on the airframe, such as wooden built-up structure with composite sandwich skin.

Given the choice of construction types, the composite structure is chosen for several reasons. First of all, the composite structure will yield a more rigid structure and a lower overall weight, especially further outboard. Also given that the wing will be designed in a CAD software, using a composite structure and skin, with a uniform material density and strength, will allow for precise estimation of weight and inertia as well as structural strength estimation. These estimates are critical for this research and cannot be performed very well for a wooden structure. In addition, given that the wing is to be designed in CAD thereby allowing for prototype testing, the need to make modifications after the build is minimized which is the largest advantage of working with wood.

C. Phase 3

1. Reynolds Number Corrections

Dynamically-scaled models were extensively used during the GA stall/spin studies in the 1970/80s.[23] Comparisons were performed against results from full-scale flight tests. The results showed that the dynamically-scaled models provided highly accurate results with regards to stalling and spin-entry characteristics but were somewhat limited due to the Reynolds number effects inherent in scaled models. Another conclusion from the studies was that a proper procedure for the scaling of Reynolds numbers was required to ensure the proper acceptance of dynamically-scaled aircraft results as a validation tool for a type-representative simulation model.

The Reynolds number effects inherent when scaling the GA-USTAR Cessna 182 model become obvious when comparisons are made for the wing airfoil (NACA 2412) aerodynamic performance curves at the stall Reynolds numbers for the full-scale and dynamically-scaled Cessna 182 shown in Fig. 6. To overcome the Reynolds number scaling issues, new wing airfoil designs are proposed for the Cessna 182 R/C model. The wing root and tip airfoil will be redesigned using the inverse airfoil design software, PROFOIL,[24,25] to match the lift and moment curve characteristics of the NACA 2412 airfoils operating at the full-scale flight Reynolds number. Given the nature of the research goals, the key matching goal here is to ensure that the lift curve shape at stall and the maximum lift point match the full-scale airfoil.

The designed airfoils will then be tested using the UIUC Low Speed Airfoil Testing experimental setup[26–30] to characterize their performance and stall characteristics at the flight Reynolds numbers of the scaled Cessna 182 model. Additional modification will be made to the airfoil (i.e., trip strips, vortex generators, etc.) to ensure that the maximum lift and stall curve closely match that of the original Cessna 182 wing airfoil (NACA 2412). The resultant airfoils will be used to build a stall-corrected dynamically scaled Cesnna 182 model to be used to validate the type-representative aerodynamic model.

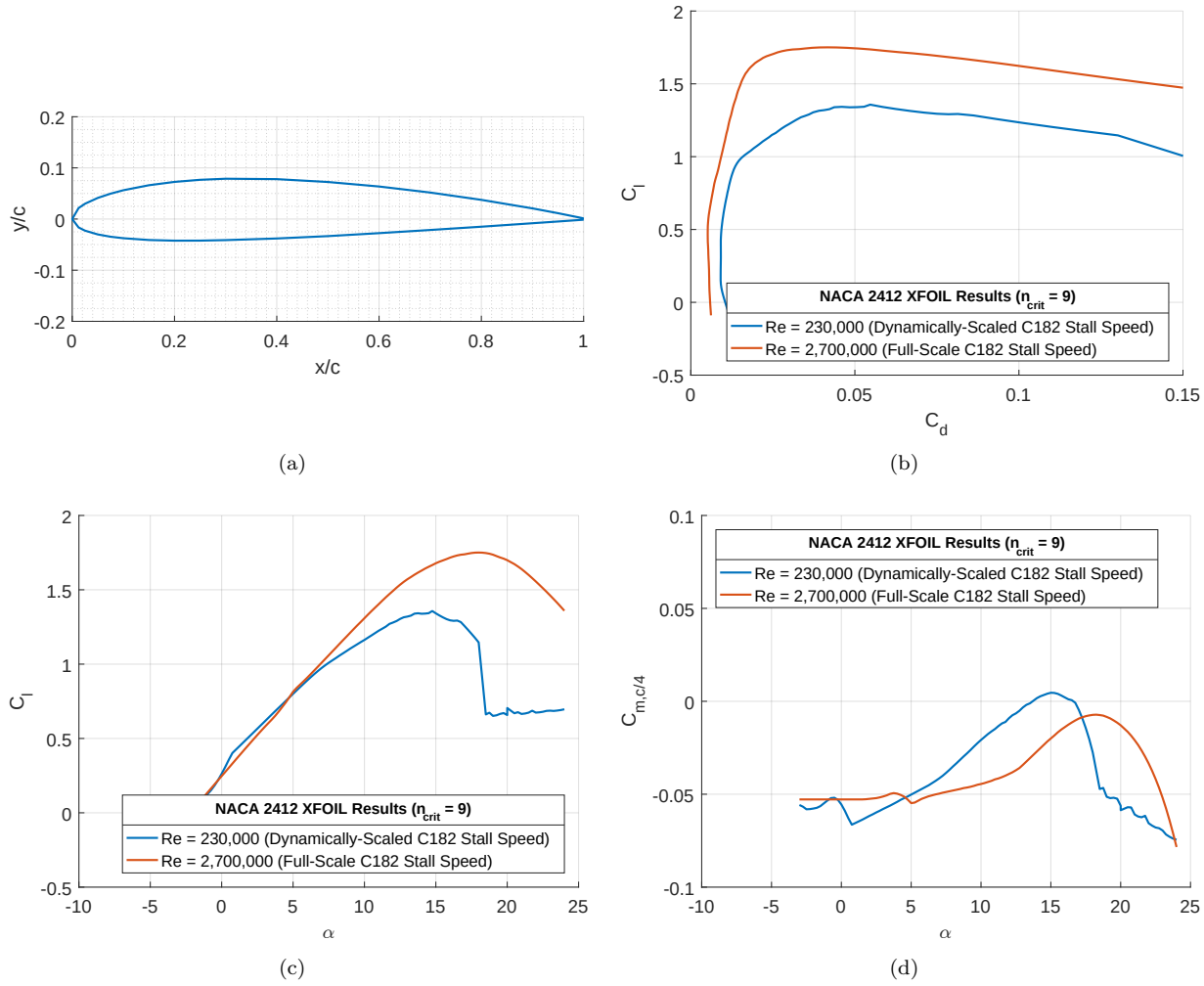

Figure 6. (a) NACA 2412 airfoil, (b) drag polar, (c) lift curve, and (d) moment curve

IV. Instrumentation and Measurement Requirements

The dynamically-scaled Cessna 182 model will be instrumented to ensure that all required flight test data are accurately measured throughout all phases of flight. Most importantly, issues relating to latency, GPS cutouts, and electromagnetic interference effects common in flight testing [18,31] should be minimized. For the current model, an Al Volo FDAQ, flight data acquistion system is used.[32] The FDAQ was specifically designed to acquire a large variety of high-fidelity state data at a rate of 400 Hz. The following flight measurements are to be made:

- linear accelerations and velocities, and positions (x, y, and z axis)
- angular rates and flight path angles (pitch, roll, and yaw / heading)
- flow conditions (angle of attack, sideslip angle, static and total pressure, ambient temperature)
- control surface deflections (aileron, flaps, elevator, and rudder deflection angles)
- motor setting (propeller RPM, voltage, current-draw)

These flight measurements will be captured by the FDAQ using a 6 degree-of-freedom inertial measurement unit with GPS receiver, a pitot-static probe, potentiometers, and pulse width modulation (PWM) signal inputs. As a result, the FDAQ will acquire and log all aircraft state, kinematic, and flow condition data in real time for the flight test maneuvers. Additional details of the integration of the flight instrumentation into the COTS R/C Cessna 182 model and flight test results is provided in a separate paper.[17]

V. Flight Test Plan

As per the FAA-published guideline bulletin regarding FSTD evaluation procedures,[1,33] the following stall entry conditions will be evaluated on the simulation model: stall entry at wings level (1g); stall entry at a constant altitude, turning flight of at least 25 deg bank angle; power-on stall entry; aircraft configurations of second segment climb, high altitude cruise (near performance-limited conditions), and approach or landing. To limit the scope of the testing, mainly power-off (wings level and turning) stalls will be tested where critical performance and handling characterisitics related to the aircraft aerodynamics such as vertical speed, pitch break, altitude loss, buffet, and uncommanded roll/yaw are to be tracked.

Prior to testing these conditions, basic flight test manuevers such as idle descent, normal climb, longitudinal trim, longitudinal maneuvering stability, longitudinal static stability, phugoid dynamics, short period dynamics, roll response (rate), spiral stability, rudder response, dutch roll, and steady-state sideslip should be tested as per published flight test guidelines and flight simulator qualification standards.[1,34,35]

VI. Conclusions

This paper discussed the development and approach taken for the UIUC GA-USTAR project. The goal of the GA-USTAR project is to provide a flight test platform to perform upset and stall maneuvers that are dynamically accurate and Reynolds number corrected for the purpose of validation of aerodynamic models developed for flight simulation. The approach taken in this project is through 3 phases. In Phase 1, a scaled COTS baseline GA aircraft model is chosen and built. The 1/5-th scale Cessna 182 was chosen due to its dynamic scalability in that minimal modifications are required to dynamically scale the aircraft. Phase 1 also involves integration of a full data acquisition systems and performing various upset and stall maneuvers. In Phase 2, the aircraft is to be dynamically scaled by performing inertia and weight scaling. A new wing will be designed for this phase. Again, in this phase, flight tests will be performed with various upset and stall maneuvers. The final and novel stage of the GA-USTAR project is Phase 3. In Phase 3, new airfoils will be designed to account for the Reynolds number effects inherent when scaling a flight model from the full size configuration. Wind tunnel tests will be performed on the newly designed wing airfoils to ensure that the aerodynamics (lift and moments) near stall closely match that of the full-scale Cessna 182 airfoil. A new final wing for the Cessna 182 model will also be built for Phase 3 and flight testing performed.

Acknowledgments

The authors would like to acknowledge the contributions of the other undergraduate members of the GA-USTAR project: Rodra Hascaryo for his detailed work on the CAD model for the Cessna 182; Mohammed Qadri for his help in inertia testing, dynamic scaling, and building the Cessna 182; and Sean Finlon for his work on the inertia testing for the Cessna 182 R/C model.

References

[1]Federal Aviation Administration, "14 CFR Part 60 : Flight Simulation Training Device Qualification Standards for Extended Envelope and Adverse Weather Event Training Tasks; Final Rule," Federal Register Vol. 81, No. 16, Department of Transportation, 2016.

[2]Federal Aviation Administration, "Qualificatin, Service, and use of Crewmembers And Aircraft Dispatchers," Rules and Regulations 78 FR 67799, Office of the Federal Register, National Archives and Records Administration, November 2013.

[3]ICAO 9625, "Manual of Criteria for the Qualification of Flight Simulation Training Devices," DOC 9625, International Civil Aviation Organization (ICAO), Montreal, Quebec, Canada, 2009.

[4]Chambers, J., *Modeling Flight: The Role of Dynamically Scaled Free-Flight Models in Support of NASA's Aerospace*

Programs, NASA, 2010.

[5]Wolowicz, C. H., Brown, J. S., Jr., and Gilbert, W. P., "Similitude Requirements and Scaling Relationships as Applied to Model Testing," NASA TP 1435, NASA, 1979.

[6]Jordan, T. L., Langford, W. M., Belcastro, C. M., Foster, J. M., Shah, G. H., Howland, G., and Kidd, R., "Development of a Dynamically Scaled Generic Transport Model Testbed for Flight Research Experiments," Tech. rep., AUVSI Unmanned Systems North America, AUVSI, Arlington, VA, 2004.

[7]Jordan, T. L., Langford, W. M., and Hill, J. S., "Airborne Subscale Transport Aircraft Research Testbed - Aircraft Model Development," AIAA Paper 2005-6432, AIAA Guidance, Navigation, and Control Conference and Exhibit, San Francisco, CA, August 2005.

[8]Bailey, R. M., Hostetler, R. W., Barnes, K. N., Belcastro, C. M., and Belcastro, C. M., "Experimental Validation: Subscale Aircraft Ground Facilities and Integrated Test Capability," AIAA Paper 2005-6433, AIAA Guidance, Navigation, and Control Conference and Exhibit, San Francisco, CA, August 2005.

[9]Cunningham, K., Foster, J. V., Morelli, E. A., and Murch, A. M., "Practical Application of a Subscale Transport Aircraft for Flight Research in Control Upset and Failure Conditions," AIAA Paper 2008-6200, AIAA Atmospheric Flight Mechanics Conference and Exhibit, Honolulu, Hawaii, August 2008.

[10]Dickes, E. G., Ralston, J. N., and Lawson, K. P., "Application of Large-Angle Data for Flight Simulation," AIAA Paper 2000-4584, AIAA Modeling and Simulation Technologies Conference and Exhibit, Denver, Colorado, August 2000.

[11]Donaldson, S., Priest, J., Cunningham, K., and Foster, J. V., "Upset Simulation and Training Initiatives for U.S. Navy Commercial Derived Aircraft," AIAA Paper 2012-4570, AIAA Modeling and Simulation Technologies Conference and Exhibit, Minneapolis, Minnesota, August 2012.

[12]National Transportation Safety Board, "Review of U.S. Civil Aviation Accidents: Review of Aircraft Accident Data 2010," NTSB ARA-12/01, Washington D.C., 2010.

[13]National Transportation Safety Board, "NTSB 2015 Most Wanted Transportation Safety Improvements: Prevent Loss of Control in Flight in General Aviation," NTSB Brochure, Washington D.C., 2015.

[14]National Transportation Safety Board, "NTSB 2016 Most Wanted Transportation Safety Improvements: Prevent Loss of Control in Flight in General Aviation," NTSB Brochure, Washington D.C., 2016.

[15]National Transportation Safety Board, "NTSB 2017 Most Wanted Transportation Safety Improvements: Prevent Loss of Control in Flight in General Aviation," NTSB Brochure, Washington D.C., 2017.

[16]Ananda, G. K. and Selig, M. S., "Stall/Post-Stall Modeling of the Longitudinal Characteristics of a General Aviation Aircraft," AIAA Paper 2016-3541, AIAA Aviation 2016, Atmospheric Flight Mechanics Conference, Washington, DC, June 2016.

[17]Dantsker, O. D., Ananda, G. K., and Selig, M. S., "GA-USTAR Phase 1: Development and Flight Testing of the Baseline Upset and Stall Research Aircraft," AIAA Paper 2017-4078, 35th AIAA Applied Aerodynamics Conference, Denver, CO, June 2017.

[18]Dantsker, O. D., Johnson, M., Selig, M. S., and Bretl, T. W., "Development and Initial Testing of the Aero Testbed: A Large-Scale Unmanned Electric Aerobatic Aircraft for Aerodynamics Research," AIAA Paper 2013-2807, 31st AIAA Applied Aerodynamics Conference, Fluid Dynamics and Co-located Conferences, San Diego, CA, June 2013.

[19]Ragheb, A. M., Dantsker, O. D., and Selig, M. S., "Stall/Spin Flight Testing with a Subscale Aerobatic Aircraft," AIAA Paper 2013-2806, AIAA 31st Applied Aerodynamics Conference, San Diego, CA, June 2013.

[20]Cunningham, K., Foster, J. V., and Shah, G. H., "GTM T1 Inertia and Center of Gravity Comparisons," GTM 6062, 2005.

[21]Torenbeek, E., *Synthesis of Subsonic Airplane Design*, Springer Science & Business Media, 1982.

[22]Roskam, J., *Airplane Flight Dynamics and Automatic Flight Controls Pt. 1*, DAR Corporation, Lawrence, KS, 2001.

[23]Chambers, J. R. and Stough, H. P., III, "Summary of NASA Stall/Spin Research for General Aviation Configurations," AIAA Paper 1986-2597, AIAA General Aviation Technology Conference, Anaheim, CA, September 1986.

[24]Selig, M. S. and Maughmer, M. D., "Generalized Multipoint Inverse Airfoil Design," *AIAA Journal*, Vol. 30, No. 11, 1992, pp. 2618–2625.

[25]Selig, M. S., *Multi-Point Inverse Design of Isolated Airfoils and Airfoils in Cascade in Incompressible Flow*, Ph.D. thesis, Dept. of Aerospace Engineering, Pennsylvania State Univ., University Park, PA, May 1992.

[26]Selig, M. S., Donovan, J. F., and Fraser, D. B., *Airfoils at Low Speeds*, Soartech 8, SoarTech Publications, Virginia Beach, VA, 1989.

[27]Selig, M. S., Guglielmo, J. J., Broeren, A. P., and Giguère, P., *Summary of Low-Speed Airfoil Data, Vol. 1*, SoarTech Publications, Virginia Beach, Virginia, 1995.

[28]Selig, M. S., Lyon, C. A., Giguère, P., Ninham, C. N., and Guglielmo, J. J., *Summary of Low-Speed Airfoil Data, Vol. 2*, SoarTech Publications, Virginia Beach, Virginia, 1996.

[29]Lyon, C. A., Broeren, A. P., Giguère, P., Gopalarathnam, A., and Selig, M. S., *Summary of Low-Speed Airfoil Data, Vol. 3*, SoarTech Publications, Virginia Beach, Virginia, 1998.

[30]Selig, M. S., *Summary of Low-Speed Airfoil Data, Vol. 4*, SoarTech Publications, Virginia Beach, Virginia, 2005.

[31]Dantsker, O. D., *Measurement of Unsteady Aerodynamic Characteristics of a Subscale Aerobatic Aircraft in High Angle-of-Attack Maneuvers*, Master's thesis, University of Illinois at Urbana-Champaign, Department of Aerospace Engineering, Urbana, IL, 2015.

[32]Al Volo LLC, "Al Volo: Flight Data Acquisition Systems," http://www.alvolo.us, Accessed Oct. 2016.

[33]Federal Aviation Administration, "FSTD Evaluation Guidelines for Full Stall Training Manoeuvres," National Simulator Program FAA AFS-205, FSTD Guidance Bulletin 14-01, 2014.

[34]Neuhart, R. A., Gingras, D. R., Hultberg, R. S., Oltman, R. S., and Graybeal, N. W., "Flight Data Collection for General Aviation Aircraft Simulation Validation," AIAA Paper 2009-5731, AIAA Atmospheric Flight Mechanics Conference, Chicago, IL, August 2009.

[35]Ward, D. T., *Introduction to Flight Test Engineering*, Kendall/Hunt, Dubuque, IA, 1996.